# Phase diagram of silicon by molecular dynamics

J. Q. Broughton
*Department of Materials Science, State University of New York at Stony Brook, Stony Brook, New York 11794-2275*

X. P. Li
*Department of Physics, State University of New York at Stony Brook, Stony Brook, New York 11794-3800*
(Received 12 January 1987)

Using the Stillinger-Weber potential we explored the liquid, crystal, and amorphous phase diagram of silicon by molecular dynamics. We obtain the chemical potential of the crystal by following the crystal-vapor coexistence curve from the $T=0$ harmonic solid up to the melting point. The liquid free energy is found by reversible expansion. The thermodynamic melting point is $1691\pm20$ K, which is very close to the experimental value of 1683 K. Contrary to experiment, the calculated supercooled liquid phase does not undergo a first-order transition to the fourfold-coordinated amorphous structure upon cooling, since the chemical potentials of these structures are almost equal over a wide range of temperatures. Diffusion coefficients, heat capacities, and expansivities are compared with experiment.

## I. INTRODUCTION

Silicon has three high-density phases at atmospheric pressures. The crystal is covalent and semiconducting, as is the amorphous phase. In contrast, the liquid is metallic, with the melting point occurring at 1683 K. Very little experimental data concerning the liquid is available mainly because of the high temperatures involved and because the melt attacks most crucibles. The amorphous structure is formed either by ion bombardment or at the very high crystal-growth rates achievable in laser annealing experiments on silicon surfaces.[1] Much of this latter data points to a first-order phase boundary separating the liquid and amorphous phases. The idea that the amorphous system is a distinct "phase" led Bagley and Chen[2] and Spaepen and Turnbull[3] to propose that the amorphous phase melts at a discrete temperature which is lower than the crystalline melting point.

Partly as a result of the paucity of data concerning the liquid and its supercooled state, attempts are presently being made to describe silicon's electronic and structural properties at the *"ab initio"* and semiempirical levels. These atomistic methods rely either upon suitably parametrized many-body interatomic potentials,[4–7] or upon phase-space trajectories based upon tight-binding or local-density-functional representations of the total energy of the system.[8–12] In many respects, silicon is proving to be the testing ground for how well we can currently predict the surface and bulk properties of matter.

Progress is well underway in the description of simply bonded systems such as the inert gases and free-electron metals. System behavior may be obtained from perturbation theories about the free-electron gas,[13] or about Lennard-Jones (LJ) reference systems[14–16] (which are in turn related to hard-sphere systems). There is no simple equivalent system for covalently bonded materials.

It is with these reasons in mind that we have explored the low-pressure phase diagram of silicon using the only potential to date that was parametrized against both liquid *and* crystalline structural data. Stillinger and Weber[4] (SW) spent much time developing this potential and it has subsequently become popular amongst surface simulationists.[17–19] The potential energy (PE) of the system is given as a sum over all pairs of atoms of a LJ-type term of depth $\epsilon$ which smoothly goes to zero at a distance $a$ (approximately the second-neighbor distance at normal densities) plus the sum over all triplets of a three-body term of the form

$$\phi_3(r_{ij},r_{ik},\theta_{jik})=\lambda\exp[\gamma(r_{ij}-a)^{-1}+\gamma(r_{ik}-a)^{-1}]\times(\cos\theta_{jik}+\tfrac{1}{3})^2 . \quad (1)$$

This term vanishes if either $r_{ij}$ or $r_{ik}$ is greater than $a$. The angular term is zero at the ideal tetrahedral angle and positive otherwise.

The purpose of this paper, then, is to determine systematically how well this potential describes the different low-pressure phases of silicon. Particularly, we are interested in its ability to distinguish between supercooled liquid and amorphous phases, since only then may molecular-dynamics (MD) be reliably used to explore growth kinetics for comparison with laser annealing studies. The normal mode spectrum, the diffusion coefficients, the heat capacities and expansivities, and the heat of fusion will be determined along the crystal-vapor and liquid-vapor coexistence lines. We will determine whether the potential can describe the amorphous phase of silicon, a system against which it was not parametrized. Further, we seek to produce a reference system against which others, described by different many-body potentials, may be compared. For this reason, we provide numerical data for the chemical potentials of the crystal and liquid phases. Simple and rapid numerical methods,[20,21] such as the "umbrella sampling" or $\lambda$-integration schemes of Monte Carlo (MC) or molecular-dynamics (MD), may then be used to relate the unknown to the SW system.

 

In Sec. II, we describe our computational method. Section III gives raw MD data for the phase diagram, including structural information and diffusion coefficients. Section IV describes the free energy analysis for the crystal and liquid. Section V compares our properties with experiment, while Sec. VI presents our conclusions.

## II. COMPUTATIONAL DETAILS

Newton's laws of motion were integrated using the Beeman[22] algorithm for a system of 512 particles with periodic boundary conditions for the crystal and liquid phases. A 216-particle system, obtained from the coordinates of Wooten, Weiner, and Weaire,[23] was used as one description of the amorphous state. Particle bookkeeping is performed, as in conventional two-body short-range potential systems, by a combination of chain-link[24] and Verlet tables.[25] Three-body forces complicate this bookkeeping only slightly. The neighbor lists are small because of the short cutoff radius of the SW potential. Properties are reported in the reduced units of the SW paper; that is, the unit of length is 0.209 51 nm, the unit of energy is $3.4723\times10^{-19}$ J and the unit of mass ($^{28}$Si) is $4.6459\times10^{-26}$ kg. The experimental triple point temperature of 1683 K is thus 0.066 89 reduced units. The reduced integration time step is 0.005.

Crystal-vapor and amorphous-vapor coexistence curves were followed by making the assumption that they are well approximated by the zero-pressure isobar. The free-energy analysis of Sec. IV will vindicate this supposition. We maintain zero pressure using the method of Broughton, Gilmer, and Weeks.[26]

## III. MOLECULAR-DYNAMICS PHASE DIAGRAM

Heating the $T=0$ crystal in small temperature increments of $\sim0.01$ for 3600 steps to equilibrate the system followed by 5000 steps to collect statistics produces the data of Figs. 1 and 2. The crystal superheats to $T=0.09$ before melting. The density ($\rho$) increases on melting as is

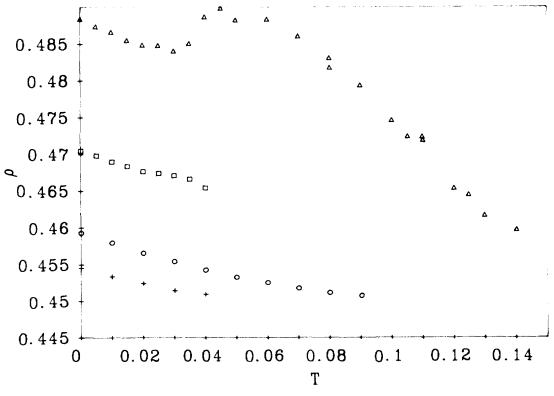


FIG. 1. Density dependence along $P=0$ isobar of the crystal (open circles), liquid (open triangles), WWW amorphous (crosses), and indirect amorphous (open squares) phases of the SW system.

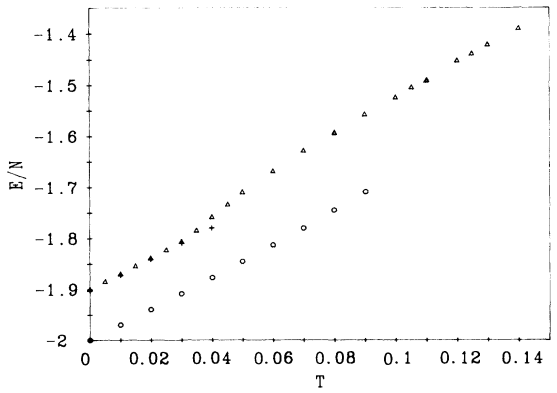


FIG. 2. Energy per particle along $P=0$ isobar of systems described in Fig. 1. The indirect amorphous system is not shown. See text.

experimentally observed. The supercooled liquid branch is obtained at temperatures below 0.07 by taking smaller temperature decrements of $\sim0.005$ and equilibrating for $\sim40\,000$ time steps before gathering statistics. The maximum in $\rho(T)$ at $T=0.045$ is quite stable, as is the minimum at $T=0.03$. For example, reheating the $T=0$ liquid, retraces essentially exactly the data obtained by cooling given in Figs. 1 and 2. Also, starting with a low-temperature disordered configuration and spontaneously heating to a temperature above 0.07 rapidly produces (i.e., within 5000 time steps) liquid configurations with energies and densities identical, within the MD noise, to those obtained by careful stepwise heating from the crystal.

The question naturally presenting itself is whether the low-$T$ disordered system is characteristic of an amorphous phase. Certainly, there is no dramatic first-order transition from the liquid into such a phase. The maximum-minimum anomaly in $\rho(T)$ coincides with a point of inflection in the $E(T)$ diagram. Thus, this temperature range is associated with a heat capacity maximum. But it is a broad maximum, the curvature of $E(T)$ away from the high-temperature linear regime occurring at temperatures above the $\rho(T)$ anomaly. The radial distribution function and the three-body correlation function (see below) change continuously throughout this temperature range.

The $\rho(T)$ anomaly seems to be related to a glass transition; diffusion becoming immeasurable on MD timescales at temperatures below 0.04. In an attempt to determine whether this SW glassy phase can be associated with amorphous silicon, we equilibrated the Wooten, Weiner, and Weaire (WWW) model of amorphous silicon[23] (which they obtain from crystalline silicon by selected displacement of atomic coordinates) at zero pressure and $T=0.03$. Cooling and reheating produces the reversible curve of Figs. 1 and 2. In keeping with experiments, the amorphous density is $\sim1\%$ lower than that of the crystal. The enthalpy difference, on the other hand, is large. (See properties section.) At temperatures above 0.04, the system undergoes a phase transition either to the liquid or to

the crystal; heating from 0.04 to 0.045 gives reproducibly the crystal phase while heating from 0.04 to 0.05 gives the liquid phase. The density in the latter case reaches the maximum in the liquid branch. Notice that whereas the densities of the supercooled liquid and amorphous phases are dissimilar, their energies are essentially identical. The free energy analysis performed in the next section shows that the driving force to amorphisation out of the supercooled liquid is extremely small.

Figure 3 gives the radial distribution functions $[g(r)]$ for the supercooled liquid and amorphous systems at a temperature of 0.03. These functions look remarkably similar except for the height of the first peak and a shoulder on the second peak of the liquid. This same shoulder exists on distribution functions obtained by rapidly quenching high-temperature liquids down to $T=0$. It is an inherent part of the structure of the liquid (observable also in Stillinger and Weber's original isochoric simulations).

As a further intercomparison, Fig. 4 gives the three-body distribution function ($g_3$) for the crystal, liquid, and amorphous systems at $T=0.03$. This gives the probability of finding an angle of ( $\cos\theta$) between triplets of particles, the bond lengths of which about the included angle are *both* less than the position of the first minimum in the $g(r)$. The crystal $g_3$ is sharply peaked about the tetrahedral angle. The amorphous system $g_3$ also peaks at this angle but the distribution is broad. On the other hand, $g_3$ of the supercooled liquid peaks at angles slightly less than tetrahedral, is broader still, and has a pronounced shoulder at approximately 84°. The essential details of this liquid distribution function are unchanged at a temperature of 0.07, in the supercooled $T=0$ liquid and in rapidly quenched liquids.

The amorphous and supercooled liquid systems appear to be distinct metastable states of the SW system. The supercooled liquid is simply the glassy state of the liquid. The three-body correlation function indicates that the glassy state is approaching a tetrahedral network and a further question to ask is whether the SW supercooled liquid is unable to find a more-stable amorphous

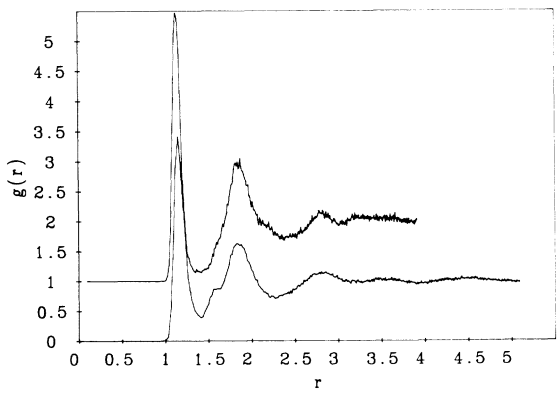


FIG. 3. Radial distribution functions of $T=0.03$ liquid (lower) and WWW amorphous systems.

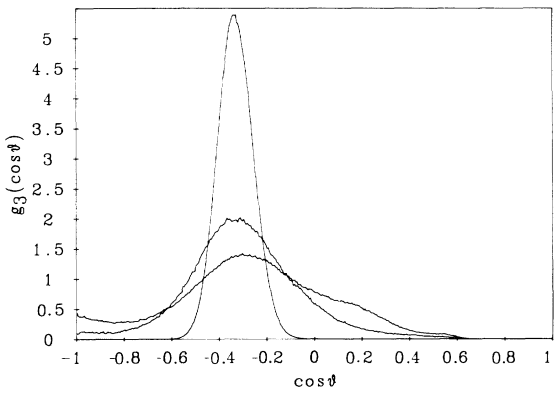


FIG. 4. Three-body correlation functions for the $T=0.03$ liquid, amorphous, and crystal systems. The liquid system has lowest maximum and broadest tail.

tetrahedral state (i.e., not necessarily that of WWW) in its sluggish exploration of phase space. One way of testing this hypothesis is to increase the strength of the three-body part of the potential to force tetrahedrality, allow the system to locally equilibrate, and then to return the potential to the SW values to see if the tetrahedral system is stable. The entire following procedure was run at zero pressure. Doubling the strength of the three-body part at a temperature of 0.05 produces a disordered system with a well-defined $g_3$ maximum about the tetrahedral angle after a run time of 10000 time steps. This system was cooled to $T=0.04$ and then to 0.03, equilibrating in each case for 10000 time steps. The potential was then returned to its SW value and the system equilibrated for 190000 time steps. Equilibration of densities and energies was very slow. Having achieved local equilibrium at this temperature, we progressed both upwards and downwards in temperature in small steps to produce the data of Fig. 1. We refer to this structure as the "indirect amorphous." Again, at low temperatures the energies of the liquid and this amorphous structure are very similar and are not plotted (for reasons of clarity) in Fig. 2. The $\rho(T)$ behavior is now midway between that of the supercooled liquid and that of WWW amorphous silicon. So too are the $g(r)$ and $g_3$ correlation functions. The indirect structure melts to the liquid at $T=0.045$. The $T=0$ value for the energy of this system is $-1.9014$ which is to be com-

TABLE I. Fraction of atoms with given coordination at $T=0.03$.

| | Fraction | | |
|---|---|---|---|
| Coordination | Liquid | WWW amorphous | Indirect amorphous |
| 3 | 0.015 | 0.012 | 0.012 |
| 4 | 0.544 | 0.866 | 0.666 |
| 5 | 0.405 | 0.118 | 0.306 |
| 6 | 0.034 | 0.002 | 0.015 |

TABLE II. Polynomials for temperature dependence of energy and density of crystal and liquid phases.

| Exponent of $T$ | Coefficient $\rho_C$ | $\rho_L$ | $E_C/N$ | $E_L/N$ |
|---|---|---|---|---|
| 0 | 0.459 280 0 | 0.463 525 1 | −2.000 000 0 | −1.899 510 0 |
| 1 | −0.143 694 6 | 1.130 482 9 | 2.994 140 6 | 2.994 140 6 |
| 2 | 0.430 458 9 | −14.780 689 | 1.303 955 9 | −7.297 969 5 |
| 3 | 1.182 408 3 | 46.342 777 | 10.027 059 | 1013.698 2 |
| 4 | | | −136.710 08 | −16 332.88 |
| 5 | | | 3800.003 4 | 98 189.462 |
| 6 | | | −19 958.824 | −207 300.11 |

pared with the relaxed WWW $T=0$ value of $-1.9022$. $E(T)$ for the WWW system and this indirect phase parallel one another extremely closely. One useful way in which to compare the supercooled liquid, WWW system and this amorphous phase is by finding the fraction of atoms with given nearest-neighbor coordination. As in the calculation of $g_3$, the radius within which neighbors are counted is the position of the first minimum in $g(r)$. Table I presents this data. In the WWW amorphous structure, fourfold coordination clearly dominates whereas in the liquid phase, the percentage of fourfold and fivefold coordination is becoming comparable. As anticipated, the coordination distribution of the indirect phase is midway between the two. It is clear that the density of the indirect structure does not conform to experimental observation (it is too dense) and in our discussion henceforth, we simply refer to the WWW structure as the amorphous phase. In conclusion, however, it is clear that the SW potential is incapable of discriminating between a wide range of low-temperature disordered structures. This of course, implies significant configurational entropies in these systems.

The $E(T)$ and $\rho(T)$ dependence of the amorphous, crystal, and liquid phases were fit to polynomials. In order to ensure correct behavior near $T=0$ (for later use in the free-energy analysis), the energies of the crystal and amorphous phases were forced to have the correct harmonic linear temperature coefficient. That this is not exactly three is a consequence of the $(3N-3)$ degrees of freedom (fixed center of gravity) of the system. The polynomials are given in Table II.

## IV. FREE-ENERGY CALCULATION

In all the ensuing, we take careful account of the degrees of freedom of the system. The MD simulations are run with fixed center of gravity. MD temperatures are obtained from the mean kinetic energy of the system; the mean here being over $3N-3$ degrees of freedom. When referencing our system to the ideal gas, we ensure that the ideal gas also has this number of degrees of freedom.

### A. Crystal

The reference state here is the $T=0$ harmonic crystal. The Helmholtz free energy of the system ($A$) is given by

$$A(T)=A_H(T)-T\int_0^T \frac{E(\tau)-E_H(\tau)d\tau}{\tau^2}, \quad (2)$$

where subscript $H$ implies the harmonic system at the $T=0$ density. For this zero-pressure system, the Helmholtz and Gibbs free energies are equal. Equation (2) was integrated using the polynomials of Table II.

The free energy of the harmonic crystal was obtained by diagonalizing the dynamical matrix. The sum of the logs of the frequencies for the 512-particle system is 4.7553 per particle. Figure 5 gives a comparison of the experimental[27] and SW-derived dispersion relationships. The agreement with experiment is extremely good except for the transverse acoustic which is well-known to be poorly described by local Keating-like potentials[28] (such as the SW). Figure 6 presents the density of states spectrum, which necessarily (given the aforementioned) agrees well with experiment. Table III gives numerical values for $A(T)$.

### B. Liquid

The natural way to determine the chemical potential of a liquid is to reversibly pull it apart and measure the work

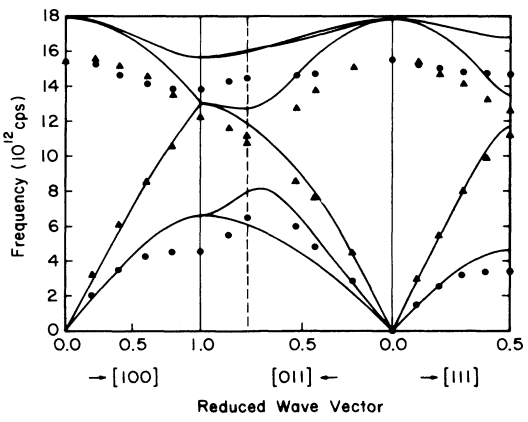


FIG. 5. Intercomparison of SW and experimental phonon dispersion curves. Points represent experiment.

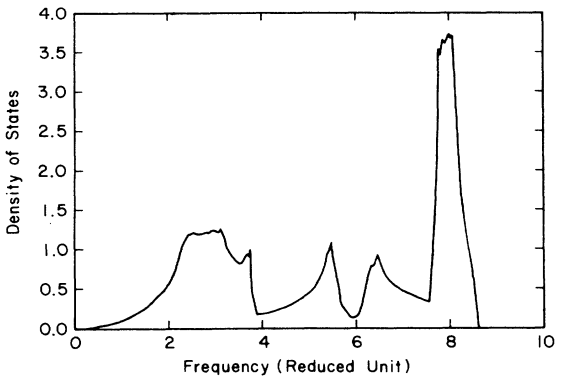


FIG. 6. Density of states of SW crystal.

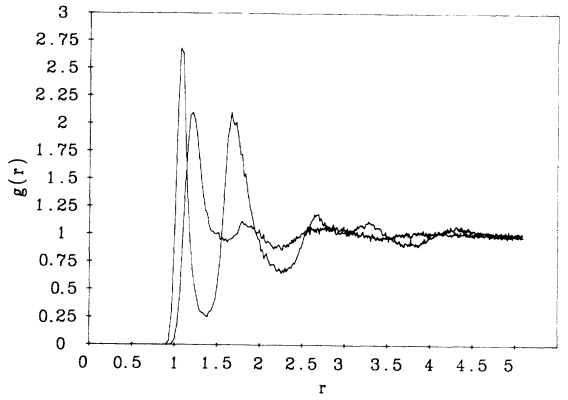


FIG. 7. Radial distribution functions of $T=0.08$ SW (lower first maximum) and repulsive potential liquids.

done. To do this with any accuracy requires that we circumvent the first-order phase boundary between the liquid and the vapor. The only attractive component of the SW potential which might stabilize a liquid-vapor interface is in the two-body part. We therefore reversibly reduce the attractive tail to zero before expanding the system to zero density.

The two-body component ($\phi_2$) which has a binding energy of 1.0 reduced units, may be written

$$\phi_2(r)=\begin{cases}\phi_{\text{rep}}(r)-1.0, & r<r_{\min}\\ \phi_{\text{att}}(r), & r>r_{\min}.\end{cases} \tag{3}$$

We rewrite this as

$$\phi_2(\lambda,r)=\begin{cases}\phi_{\text{rep}}(r)-1.0+\lambda, & r<r_{\min}\\ (1-\lambda)\phi_{\text{att}}(r), & r>r_{\min},\end{cases} \tag{4}$$

where $\lambda$ now is the integration parameter and "rep" and "att" represent repulsive and attractive parts of the potential. This way of decomposing a potential into its repulsive and attractive component parts is the basis of the Weeks-Chandler-Andersen[14,15] perturbation theory of liquids. For simple liquids described by a two-body potential with a slowly varying attractive tail, the structure of the liquid is almost independent of the presence (or otherwise) of the tail provided the density of the system is held constant.

We used Eq. (4) to drive the dynamics of our system at seven values of $\lambda$ ranging from 0 to 1. We evaluate, at each value $(\partial E/\partial\lambda)$ since the Helmholtz free-energy difference between the Stillinger-Weber state and the repulsive state ($\lambda=1$) is given by

$$\Delta A=\int_0^1(\partial E/\partial\lambda)d\lambda\ . \tag{5}$$

The $\lambda$ integration was performed at a temperature close to our expected melting point. We chose $T=0.08$. The density of the system was fixed at the value given by the $\rho(T)$ liquid polynomial for this temperature. The plot of $(\partial E/\partial\lambda)$ has a gentle point of inflection but is almost linear. The polynomial fit to this data is given in Table IV. Figure 7 illustrates the change in structure that occurs upon going from $\lambda=0$ to 1. The first peak of the $g(r)$ moves toward the origin and the second-neighbor peak becomes very intense. We see that the attractive tail of the two-body potential is very important in determin-

TABLE III. Chemical potentials of crystal, amorphous, and liquid phases. The term of order 3 $kT\ln\hbar$ is omitted.

| Temperature | Crystal | Liquid | Amorphous |
|---|---|---|---|
| 0.00 | −2.0000 | −1.8995 | −1.9022 |
| 0.01 | −1.8147 | −1.7239 | −1.7204 |
| 0.02 | −1.6712 | −1.5908 | −1.5805 |
| 0.03 | −1.5437 | −1.4756 | −1.4568 |
| 0.04 | −1.4266 | −1.3736 | −1.3437 |
| 0.05 | −1.3176 | −1.2821 | |
| 0.06 | −1.2150 | −1.1995 | |
| 0.0672 | −1.1446 | −1.1446 | |
| 0.07 | −1.1179 | −1.1241 | |
| 0.08 | | −1.0547 | |
| 0.09 | | −0.9902 | |
| 0.10 | | −0.9296 | |

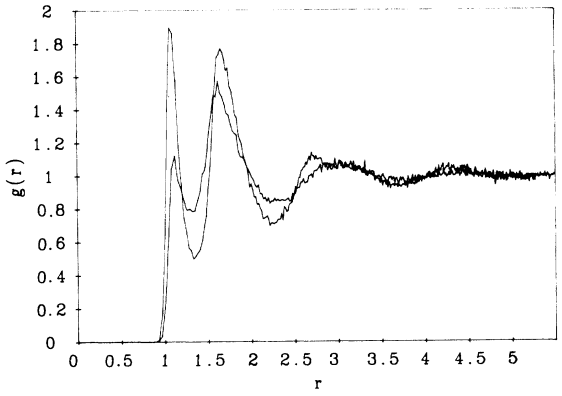


FIG. 8. Radial distribution functions of $T=0.08$ low density ($\rho=0.435$ and 0.345) repulsive potential liquids. See text.

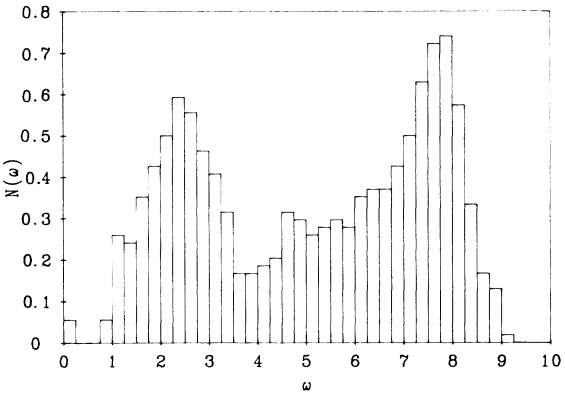


FIG. 9. Density of states of SW WWW-amorphous phase.

ing the liquid's structure.

Lastly, we integrate $(P/\rho^2)d\rho$ as the repulsive liquid is expanded to infinite value. The system is well behaved with no phase transitions. At high densities, 4000 time steps were used for equilibrium followed by 5000 time steps for accumulating statistics. At low density, this was increased by a factor of 4 to account for the lower collision rates. Figure 8 shows that as the density is decreased, the second-neighbor $g(r)$ peak increases in intensity at the expense of the first-neighbor peak. In order to facilitate integration of the pressure data, we also calculated the value of the second Virial coefficient and used this in the fit of the data to a polynomial. The polynomial is given in Table IV, and values for $A(T)$ along the liquid $P=0$ isobar are given in Table III.

### C. Amorphous system

Proceeding as for the crystal-free energy, we find that the sum of the logs of the frequencies per particle for the relaxed Wooten-Weiner-Weaire (WWW) 216-particle system is 4.4546. Since the entropy of a harmonic system is proportional to the inverse of this quantity we find that the vibrational entropy of the amorphous system is higher than that of the crystal. The density of states spectrum is shown in Fig. 9. It is necessarily coarser than that of the crystal, since only the $k=0$ state was computed. (Periodic replication of an amorphous system has no meaning.) The chemical potential of the system was computed from Eq. (2) and numerical values are presented in Table III.

The data for the low-temperature liquid and amorphous phases are in error, of course, by the configurational entropy. Given that the SW potential produces a range of degenerate disordered structures, we assume that this term is of similar magnitude in each disordered phase. Whatever the magnitude, however, it is clear that the heat of fusion of the amorphous to liquid transition is much too small relative to experiment.[29,30] Further, it is clear that the driving force to *amorphization* out of the liquid state is so small within the SW framework that no such transition is seen on MD time scales.

## V. PROPERTIES

In the previous section we have seen how well the SW potential fits experimental phonon dispersion curves. The

TABLE IV. Polynomials for $(\partial E/\partial\lambda)(\lambda)$, $P_{\text{rep}}(\rho)$, and $E_A/N(T)$ and $\rho_A(T)$.

| | Coefficient | | | |
|---|---|---|---|---|
| Exponent | $(\partial E/\partial\lambda)$ | $P_{\text{rep}}$ | $E_A/N$ | $\rho_A$ |
| 0 | 2.363 633 1 | 0.0 | −1.902 250 0 | 0.454 530 0 |
| 1 | −0.928 128 9 | 0.079 843 7 | 2.986 111 1 | −0.127 914 5 |
| 2 | 0.643 051 6 | 0.195 143 2 | 2.566 948 3 | 0.920 805 5 |
| 3 | −0.228 756 7 | 1.795 345 3 | | |
| 4 | | 23.096 827 | | |
| 6 | | −695.032 21 | | |
| 7 | | 7861.456 3 | | |
| 8 | | −42 675.661 | | |
| 9 | | 122 866.41 | | |
| 10 | | −178 095.68 | | |
| 11 | | 101 777.27 | | |

TABLE V. Triple-point properties.

| | Simulation | Experiment[a] |
|---|---|---|
| $T_m$ (K) | 1691 | 1683 |
| $D$ ($cm^2 s^{-1}$) | $6.94\times10^{-5}$ | $\sim10^{-4}$ |
| $L_{CL}$ ($J mol^{-1}$) | $30.9\times10^{3}$ | $50.6\times10^{3}$ |
| $\rho_C$ ($g cm^{-3}$) | 2.283 | 2.40 |
| $\rho_L$ ($g cm^{-3}$) | 2.459 | 2.53 |
| $P$ (Pa) | 0.309 | $\sim0.1$ |
| $C_{P_C}$ ($Jg^{-1} K^{-1}$) | 0.999 | 1.04 |
| $C_{P_L}$ ($Jg^{-1}K^{-1}$) | 1.256 | 1.04 |
| $X_C$ ($K^{-1}$) | $2.047\times10^{-6}$ | $4.4\times10^{-6}$ |
| $X_L$ ($K^{-1}$) | $6.210\times10^{-6}$ | $5.2\times10^{-5}$ |

[a]Reference 35.

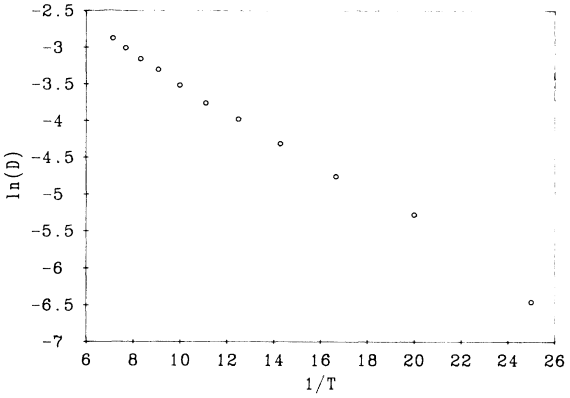


FIG. 10. Arrhenius plot of diffusion coefficient behavior.

other low temperature property of interest is the latent heat ($L$) of crystallization out of the amorphous phase. Donovan *et al.*[29] calorimetrically measured 20 samples of amorphous silicon prepared by different methods to arrive at a value of $11.3\pm0.8$ kJ/mole. In contrast, we find a value of 20.4 kJ/mole which is approximately constant over the temperature range of stability of our WWW system. The SW potential therefore significantly overestimates this quantity. In contrast, the latent heat differences between the liquid and amorphous phases will be given experimentally as the difference (approximately) between the heat of the amorphous to crystalline transition and the heat of fusion; that is, approximately 39 kJ/mole.[31] Comparing this quantity with our system is indirect since our amorphous phase is not stable up to the experimentally ascertained amorphous-liquid melting point of $\sim1480$ K.[32] At low temperatures, our $L_{AL}$ is extremely small whereas a value extrapolated, very crudely using Fig. 2, to 1480 K yields 9.6 kJ/mole. In either case, the SW value is lower than experiment.

Turning now to triple point properties, these are listed in Table V. The melting point is in extraordinarily good agreement with experiment while the latent heat achieves approximately $\frac{2}{3}$ of the experimental value. The thermodynamically derived $T_m$ is midway between the values found by Abraham and Broughton[18] and by Landman and co-workers[17] in their two-phase coexistence calculations using the SW potential. Densities and equilibrium vapor pressures are in tolerable agreement with experiment. In fact, it is this low-vapor pressure which vindicates our choice of zero pressure for these bulk phase MD calculations. Heat capacities ($C_P$) are really in very close agreement with experiment while expansivities ($X$) are within an order of magnitude of being correct. Lastly, the diffusion coefficient ($D$) is in reasonable agreement with the value that many authors guess to be that of liquid silicon. (It is usually assumed that the self-diffusion coefficient is of the same order as that of common dopants in liquid silicon.)[33] An Arrhenius plot of diffusion coefficients, obtained from the Einstein relation relating mean-square displacements with $D$, is shown in Fig. 10. All in all, the SW potential reproduces triple-point properties really rather well.

## VI. CONCLUSIONS

We may summarize simply by saying that the SW potential does rather well at obtaining triple-point properties of the crystal and liquid phases and $T=0$ properties of the crystal but that the thermodynamics of the amorphous phase is poorly described. In fact, it predicts a melting point below room temperature which is very different from the experimentally derived value of $\sim1480$ K.[32] That the potential imperfectly handles the three different phases simultaneously is in accord with a recent publication of Ding and Andersen[34] who studied liquid and amorphous germanium using a SW-like potential. They showed that parametrization to achieve a good amorphous $g(r)$ produces a poor analogous distribution function for the liquid. Lastly, we find that the SW supercooled liquid structure represents a glassy extension of the liquid which is dissimilar from WWW amorphous silicon. Attempts to quench a SW liquid directly into an amorphous structure failed.

## ACKNOWLEDGMENT

We thank U. S. Department of Energy (DOE) for its support of this work (under Contract No. DE-FG02-85ER45218).

[1]J. M. Poate, in Proceedings of the MRS Symposia on Laser and Electron-Beam Interactions with Solids, edited by B. R. Appleton and G. K. Celler, 1982, Vol. 4 (unpublished).

[2]B. G. Bagley and H. S. Chen, *Laser Solid Interactions and Laser Processing*, Proceedings of the Conference on Laser Solid Interactions and Laser Processing, AIP Conf. Proc. No. 50, edited by S. D. Ferris, H. J. Leamy, and J. M. Poate (AIP, New York, 1978).

[3]F. Spaepen and D. Turnbull, *Laser Solid Interactions and Laser Processing*, Proceedings of the Conference on Laser Solid Interactions and Laser Processing, AIP Conf. Proc. No. 50, edited by S. D. Ferris, H. J. Leamy, and J. M. Poate (AIP, New York, 1978).

[4]F. H. Stillinger and T. A. Weber, Phys. Rev. B 31, 5262 (1985).

[5]E. Pearson, T. Takai, T. Halicioglu, and W. A. Tiller, J. Cryst. Growth **70**, 33 (1984).
[6]R. Biswas and D. R. Hamann, Phys. Rev. Lett. **55**, 2001 (1985).
[7]J. Tersoff, Phys. Rev. Lett. **56**, 632 (1986).
[8]O. F. Sankey and R. E. Allen, Phys. Rev. B **33**, 7164 (1986).
[9]M. Menon and R. E. Allen, Phys. Rev. B **33**, 7099 (1986).
[10]R. Car and M. Parrinello, Phys. Rev. Lett. **55**, 2471 (1985).
[11]P. B. Allen, J. Q. Broughton, and A. K. McMahan, Phys. Rev. B **34**, 859 (1986).
[12]J. Q. Broughton and P. B. Allen, in Proceedings of the MRS Symposia on Computer-Based Microscopic Description of the Structure and Properties of Materials, edited by J. Broughton, W. Krakow, and S. T. Pantelides, 1986, Vol. 63 (unpublished).
[13]W. A. Harrison, in *Pseudopotentials in the Theory of Metals* (Benjamin, 1966).
[14]J. D. Weeks, D. Chandler, and H. C. Andersen, J. Chem. Phys. **54**, 5237 (1971).
[15]H. C. Andersen, J. D. Weeks, and D. Chandler, Phys. Rev. A **4**, 1597 (1971).
[16]J. A. Barker and D. Henderson, J. Chem. Phys. **47**, 4714 (1967).
[17]U. Landman, W. D. Luedtke, R. N. Barnett, C. L. Cleveland, M. W. Ribarsky, E. Arnold, S. Ramesh, H. Baumgart, A. Martinez, and B. Khan, Phys. Rev. Lett. **56**, 155 (1986).
[18]F. F. Abraham and J. Q. Broughton, Phys. Rev. Lett. **56**, 734 (1986).
[19]F. F. Abraham and I. P. Batra, Surf. Sci. **163**, L752 (1985).
[20]G. Torrie and J. P. Valleau, J. Comp. Phys. **23**, 187 (1977).
[21]C. H. Bennett, J. Comp. Phys. **22**, 245 (1976).
[22]D. Beeman, J. Comp. Phys. **2**, 130 (1976).
[23]F. Wooten, K. Winer, and D. Weaire, Phys. Rev. Lett. **54**, 1392 (1985).
[24]B. Quentrec and C. Brot, J. Comp. Phys. **1**, 430 (1973).
[25]L. Verlet, Phys. Rev. **159**, 98 (1967).
[26]J. Q. Broughton, G. H. Gilmer, and J. D. Weeks, J. Chem. Phys. **75**, 5128 (1981).
[27]G. Nilsson and G. Nelin, Phys. Rev. B **6**, 3777 (1972).
[28]P. N. Keating, Phys. Rev. **145**, 637 (1966).
[29]E. P. Donovan, F. Spaepen, D. Turnbull, J. M. Poate, and D. C. Jacobson, J. Appl. Phys. **57**, 1795 (1985).
[30]D. Turnbull, in Proceedings of the MRS Symposia on Beam-Solid Interactions and Phase Transformations, edited by H. Kurz, G. L. Olson, and J. M. Poate, New York, 1986, Vol. 51 (unpublished).
[31]H. F. Wolf, *Silicon Semiconductor Data, International Series of Monographs on Semiconductors* (Pergamon, New York, 1969), Vol. 9.
[32]M. O. Thompson, G. J. Galvin, J. W. Mayer, P. S. Peercy, J. M. Poate, D. C. Jacobson, A. G. Cullis, and N. Chew, Phys. Rev. Lett. **52**, 2360 (1984).
[33]For example, see many of the papers in Refs. 1, 2, and 30.
[34]K. Ding and H. C. Andersen, Phys. Rev. B **34**, 6987 (1986).
[35]Experimental data compiled from V. M. Glozov, S. N. Chizhevskaya, and N. N. Glagoleva, *Liquid Semiconductors* (Plenum, New York, 1969); *Semiconductors: Technology of Si, Ge, and SiC,* Vol. III/17 of *Landolt-Börnstein,* edited by EDITOR (Springer-Verlag, New York, 1984); Y. S. Touloukian and E. H. Buyco, *Thermophysical Properties of Matter* (Plenum, New York, 1970), Vol. 4; Y. S. Touloukian, R. K. Kirby, R. E. Taylor, and T. Y. R. Lee, *Thermophysical Properties of Matter* (Plenum, New York, 1977), Vol. 13.